

Seismic Performance Evaluation of a Six Story Inner Frame Supported Masonry Building Based on In-Situ Impact Test

Peizhou Zhang, Shuang Hou & Jinping Ou

School of Civil Engineering, Dalian University of Technology, Dalian, China



SUMMARY:

Inner frame-supported masonry building is a typical and widely used structure form in China during 1970s and 1980s, with poor seismic performance during previous earthquakes. To investigate such structures' seismic performance, we choose a six-story building from the 1980s for the research. Firstly, an in-situ impact test is applied to the structure continuously to create various damage states. Secondly, a finite element model is created in ABAQUS, and updated based on measured experimental data to approach the realistic model. Finally, by fitting the response spectrum of Chinese Code for Seismic Design of Buildings, three earthquake waves were selected in nonlinear time-history analysis to the finite model, and then the seismic capability and failure mode of this structure form is discussed. The results show that for most of such structures the first stories are the weak stories, and their seismic capabilities are not satisfied with the current code under severe earthquakes.

Keywords: inner frame-supported masonry structure, in situ test, seismic performance

1. INTRODUCTION

Frame-supported masonry buildings, especially inner frame-supported masonry buildings had been widely built on street sides for business purpose in 1970s' and 1980s' China. They are usually used as residential-commercial hybrid, with a low compressive concrete strength and drastically changed vertical stiffness (Zhou, 2009), which lead to their poor seismic performance during previous earthquakes, such as Wenchuan earthquake. To investigate this type of structure's seismic performance, a six-story building from 1980s is chosen for an in-situ impact test, during which its dynamic characteristics under various damage states are measured for later research. Such a large in-suit test is really rare around the world and its results are constructive for researches.

2. DESCRIPTION OF STRUCTURE AND IMPACT TEST

2.1. Brief Introduction of the Structure

The six-story structure was built in 1980s, and located in Dalian, China. The first story is 3.5 meters high, with cast-in-place R.C. slab, supported by R.C. frames inside and brick walls outside, mainly used for business purposes; other stories are 3.0 meters high, with precast R.C. slabs, supported by only brick walls, mainly used as residences; as shown in Fig. 2.1 and Fig. 2.2.

Measured data shows the average of concrete strength is only 20 MPa, the stirrups are $\Phi 6$, and at the stirrup densified regions the stirrup spacing is 200mm. Both the concrete compressive strength and the stirrup ratio are fairly low, which don't meet the demand of current Chinese seismic code (GB 50011-2010, 2010).



Figure 2.1. Inner frame-supported masonry structure

Figure 2.2. Columns of the inner frame

2.2. Impact Test Description

The horizontal impulse load is applied by a gravity hammer at the height of the first floor as shown in Fig. 2.3. During the whole test process, the load mentioned above has been applied first to the left side of the structure several times, then to right side, at last to the back of it until it collapses. Fig. 2.6 describes several test conditions of the experiment. The measuring instruments include smart aggregates (SA), accelerometers and dynamic inclinometers. SA, which made of piezoelectric material, is developed by our research group to monitor the value of concrete stress changes under dynamic load (Hou et al, 2010). In the test, 2 SAs are used to measure shear stresses of beam-column joints, 14 SAs for normal concrete stresses at the ends of column 3 and column 4; 3 accelerometers for horizontal accelerations of the joints and the impact point; 5 dynamic inclinometers for the rotation angles of the joints and the cross sections at the ends of columns. The layouts of all sensors in the structure are shown in Fig. 2.5, Fig. 2.7 and Fig. 2.8. Data acquisition equipment is located about 30 meters away from the structure for safety, and about 1200 meters wires are used as shown in Fig. 2.4.



Figure 2.3. Impulse load

Figure 2.4. 1200 meters wires

Figure 2.5. Sensors in the structure

2.3. Material Properties

Before the test, four groups of concrete cylinder with diameter 75.5mm were taken from less important beams as specimens, also two groups of longitudinal reinforcements were taken from a beam and a column as specimens. The average of concrete strength and steel strength are given in Tab 2.1 and Tab 2.2.

Table 2.1. Average of Concrete Strength

Concrete	d/mm	h/mm	f_c /MPa
Average	75.75	77.75	20.5

Table 2.2. Average of Strength

Location of Steel	d/mm	ϵ_y	f_y /MPa	f_u /MPa
Beam	18	0.002	437.5	607.5
Column	20	0.002	410.0	582.5

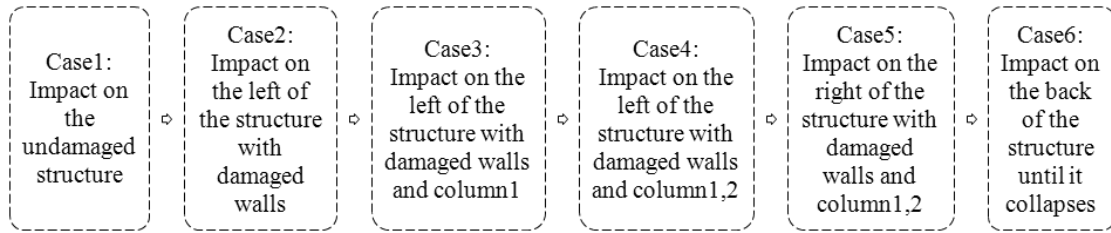


Figure 2.6. Description of test conditions

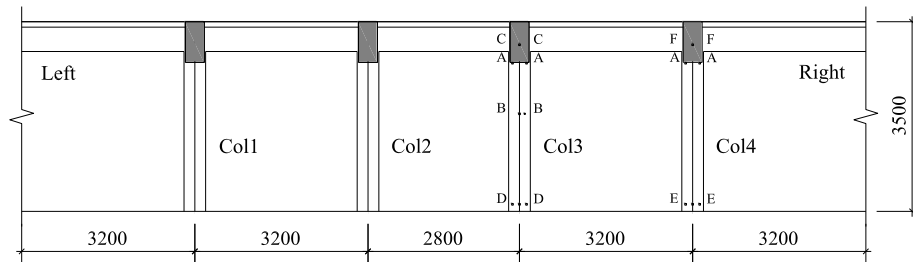


Figure 2.7. Sensors on the inner frame (Section 1-1 in Figure 2.9)

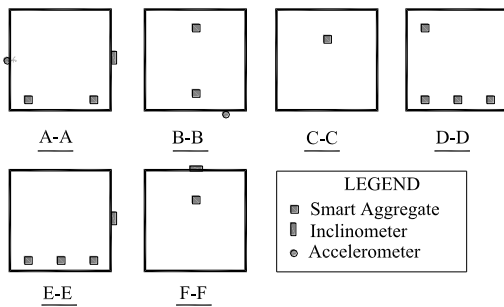


Figure 2.8. Sensors in the cross sections

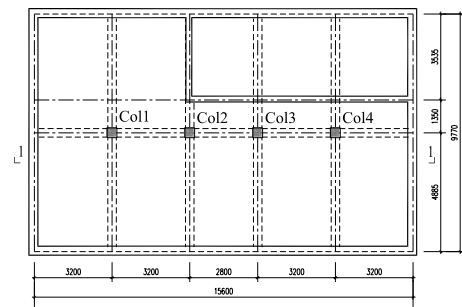


Figure 2.9. Structural plan of the first floor

3. ANALYSIS OF TEST RESULTS

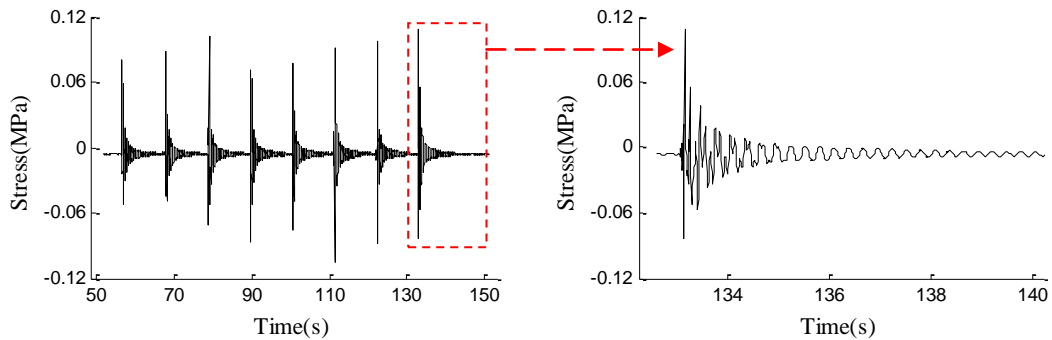


Figure 3.1. Values of stress changes measured with SA in the joint of column 3

This part focus on study the damage evolution process with measured data of the structure under all damage states from the test mentioned above. Fig. 3.1 shows the values of stress changes measured

with SA in the joint of column 3 during multiple impacts.

3.1. Structural dynamic characteristics

3.1.1. Changes of frequency

The structural frequencies of test condition case1 to case4 (Fig. 2.6) are shown in Fig. 4.7 and Fig. 4.8, which are obtained with transfer function method based on the SA data. The figures show that when the damage is small or local, the changes of the damage won't cause serious impact on structural frequency, which changes no more than 3.6% before and after the failure of column 1.

3.1.2. Changes of damping ratio

Damping ratio determines the decay rate of structural vibration during free vibration. It is one of structural dynamic characteristics, which depends on the mass and stiffness of the system. In this test, we use free vibration method to obtain the damping ratios ξ under different damage states, which is calculated according to the formulation 3.1 below:

$$\xi = \frac{v_n - v_{n+m}}{2\pi m v_{n+m}} \quad (3.1)$$

where v_n and v_{n+m} mean two amplitudes m cycles apart.

The structural damping ratios during the multiple impacts from test condition case1 to case2 are calculated according to the formulation above, and shown in Fig. 3.2. The figure shows that with the damage increases, the overall trend of damping ratio is increasing gradually, while the jagged fluctuations are due to experimental errors and the discreteness of selected data. To the undamaged structure, damping ratio is only 1.6%, very different from the commonly used 5%, which may cause great difference on the results of structural seismic response analysis.

3.2. Evolution of structural damage

The structure has been hit more than a hundred times during the entire experiment, and each time the structural damage increases. The trend of structural frequency during the first 40 impacts is obtained through frequency recognition and is shown in Fig. 3.3, where ordinate refers to the ratio of the structural frequency after certain impact to that of the undamaged structure, and abscissa refers to the number of impacts. The jagged fluctuations are caused by experimental errors. The figure shows that the natural frequency of structure decreases when the damage increases, but within a small range. The results can be applied to update the finite element model.

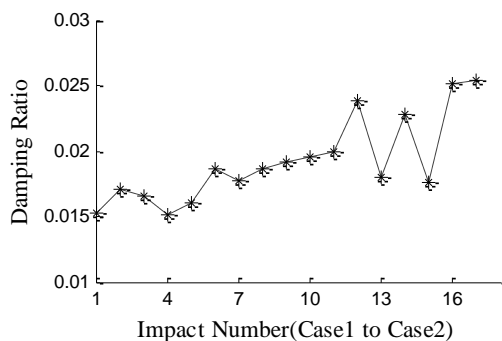


Figure 3.2. Trend of structural damping ratio from test case1 to case2

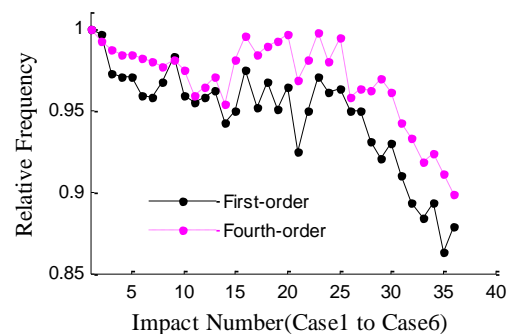


Figure 3.3. Trend of structural frequency during the first 40 impacts

4. STRUCTURAL MODEL UPDATING

4.1. Modeling of structure

Due to high discreteness of masonry material, complexity of construction measures and relatively low calculation efficiency, it's very difficult to model the entire frame-supported masonry structure, especially for the seismic nonlinear analysis purpose. However, it's necessary to understand the structure's nonlinear and collapse behavior under severe earthquakes when assessing seismic performance. For inner frame-supported masonry structures, the vertical stiffness changes drastically, and the resistance to lateral force of different frames varies greatly. As a result, such structures tend to have one or more weak stories, and for the structure we study in this paper, the weak story may be the first story. Thus, when modeling in ABAQUS, the frames and walls of the first story are meshed more intensively, and the material property adopts the ABAQUS-embedded concrete damage plasticity constitutive model. Other stories are meshed less intensively and only the elastic stiffness of the walls is considered. The meshing of the structure is shown in Fig. 4.2. It is assumed that flexural stiffness of the slabs is infinite in the plane, and bearing walls would fail prior to connecting elements.

The model's external wall is 370mm thick, and the internal wall is 240mm thick. As shown in Fig. 4.1, the first story is supported by R.C. frame inside and brick walls outside, while the other stories are supported by only brick walls. Concrete: measured strength 20MPa, brick wall: a combination of Mu10 and M7.5, steel reinforcement: yield strength 438MPa (in beams) and 410MPa (in columns).

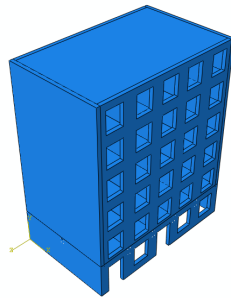


Figure 4.1. Numerical model of the structure

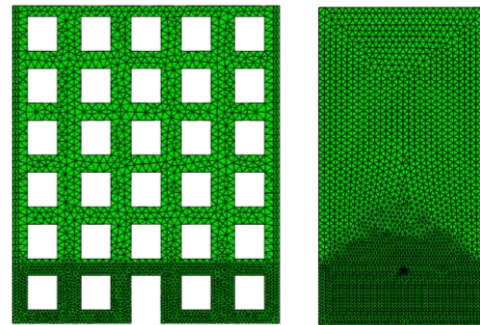


Figure 4.2. Mesh of structure

The constitutive relationship recommended by Chinese Code for Design of Concrete Structures is applied to simulate concrete, while the constitutive relationship in Zheng's paper is used to simulate brick walls. Fig. 4.3 and Fig. 4.4 show the stress-strain relationships of concrete and brick walls respectively.

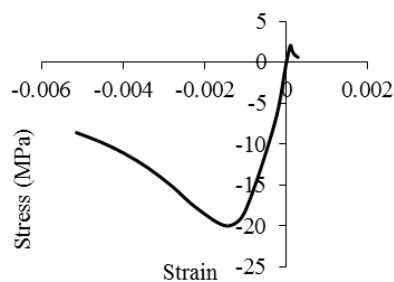


Figure 4.3. Stress-strain relationship of concrete

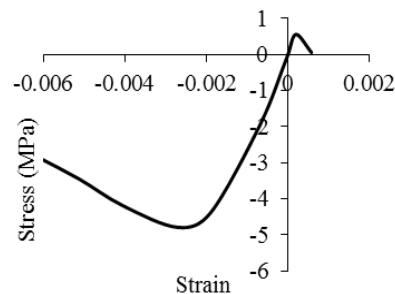


Figure 4.4. Stress-strain relationship of brick walls

4.2. Numerical model updating

The structure is modeled in ABAQUS based on its actual information from the site survey, and then a modal analysis is conducted. The first four mode shapes are shown in Fig. 4.5. Compared with the

measured frequencies mentioned above, the conclusion can be drawn that the modes excited during the test are the first and the fourth order mode.

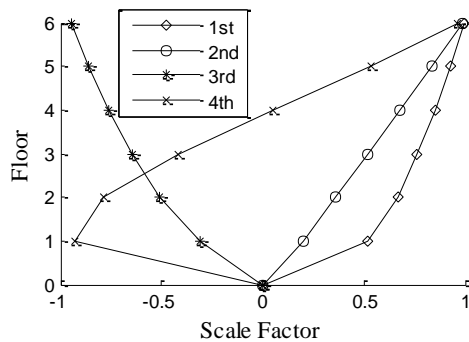


Figure 4.5. First four order mode shapes of the undamaged structure (case1)

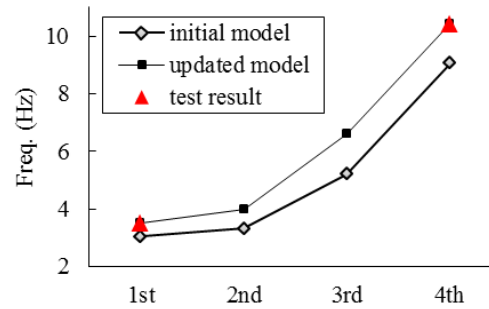


Figure 4.6. Frequencies of the test results, updated model and initial model under undamaged state (case1)

The results of the initial model in Fig. 4.6 represent the first four frequencies calculated with the initial model, which have significant differences compared with the test results. One possible reason is that from the second story to the top the structure is residentially used with more complicated situation, so the site survey may not be detailed enough for an accurate simulation. Moreover, the discreteness of the masonry materials may lead to inaccurate material parameters in modeling. So under the certain structural mass, the numerical model could be updated by changing the stiffness matrix and the material parameters on the basis of experimental data under undamaged state, until structural natural frequency agrees well with the experimental result (shown as results of updated model in Fig. 4.6). Finally the updated model can be validated by frequency comparison between test results and simulation results under other damage states.

The objective of updating the model is to make it closer to the actual structure and to do further structural analysis with it. To illustrate the effectiveness of this method, the first and fourth frequencies of the test results and updated model under different damage states are shown in Fig. 4.7 and Fig. 4.8. In Fig. 4.7, the first frequency of the test results under undamaged state (case1) is the reference used to update the model, and we can see from Fig. 4.8 the model's fourth frequency automatically matches with the test result. The model's frequencies under other damaged states (case2 to case4) are gained through simulation to the impulse load process. The figures show that the model's frequencies match well with the test results, with the error less than 5%, which is shown in Fig. 4.9.

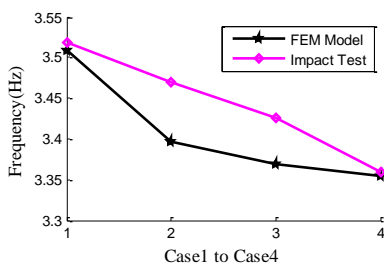


Figure 4.7. First-order frequency under different damage states

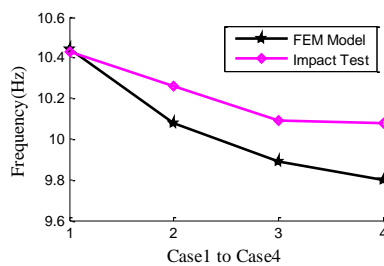


Figure 4.8. Fourth-order frequency under different damage states

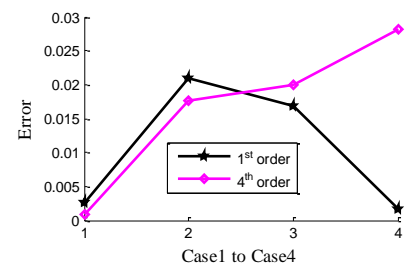


Figure 4.9. Errors of first and fourth order frequencies

5. SEISMIC PERFORMANCE ANALYSIS

5.1. Time-History Analyses

NorthRidge wave, El-centro_NS wave and Loma_Prieta wave are modified with SeismoMatch to fit

the code response spectrum as shown in Fig. 5.1, and then applied to the model as input ground motions. In this case, the structure is built at field sort II, designed to resist 7 degrees intensity earthquakes, so the parameters of the code response spectrum (GB 50011-2010, 2010) are as followed: the horizontal seismic coefficient is 0.5; the characteristic period of the field is 0.35s. The comparison between the modified waves spectrums and code response spectrum is shown in Fig. 5.2, from which we can see the mean response spectrum of the three waves agrees reasonably well with the target one.

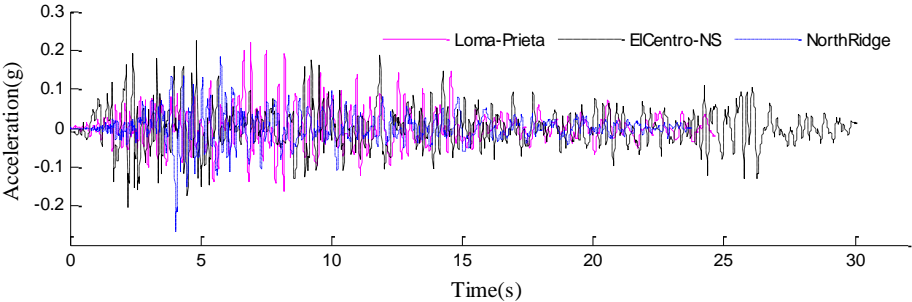


Figure 5.1. Modified time-history curves of selected earthquake waves

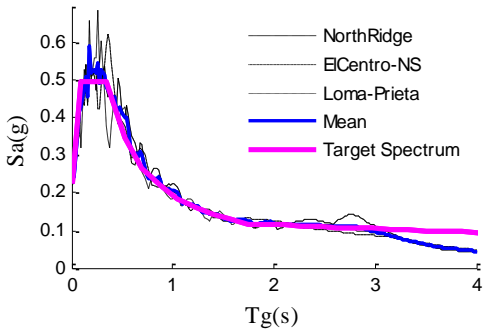


Figure 5.2. Modified response spectrum of selected earthquake waves compared with the target one

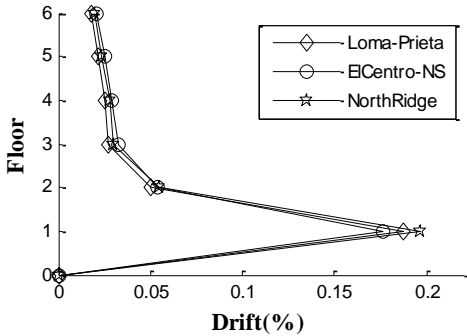


Figure 5.3. Distribution of maximum story drift under earthquakes

The time-displacements (2s~11s) at the top of the building from nonlinear time-history analyses with Rayleigh damping are shown in Fig. 5.4. The maximum displacements of the structure under three seismic waves are 11.02mm, 11.92mm and 11.83mm.

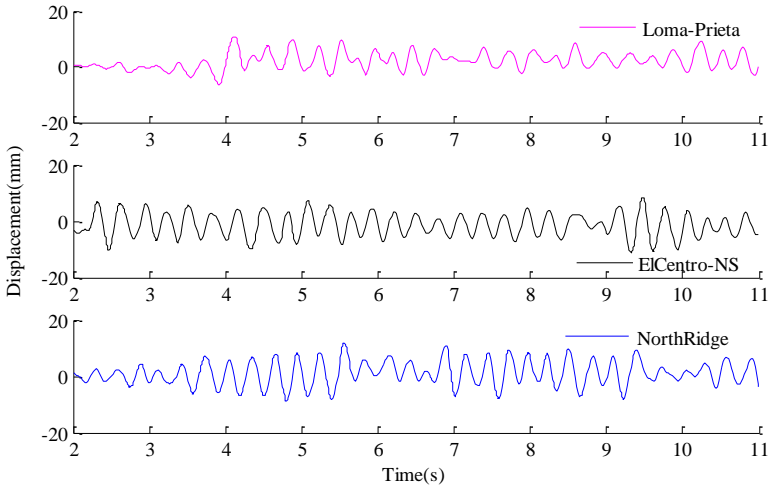
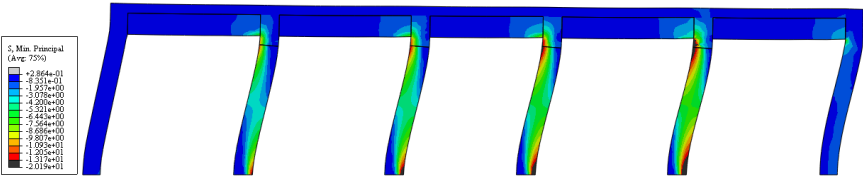


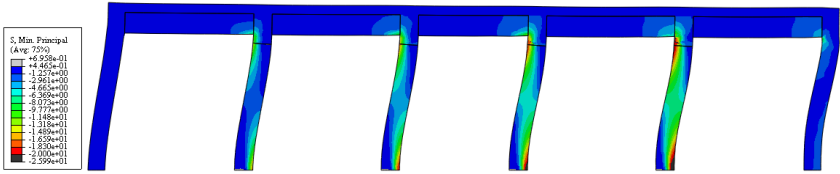
Figure 5.4. Time-displacement of the structure under seismic waves

5.2. Failure Mode Analyses

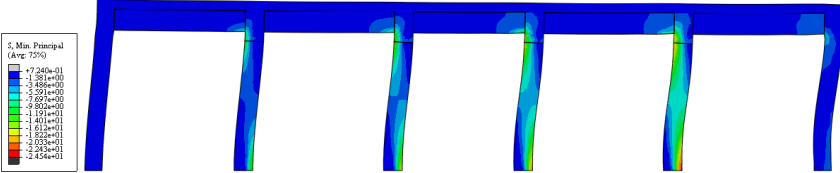
Fig. 5.5 are the stress contours of the inner frame under three earthquake waves at the onset of maximum stress in the inner frame. The stresses at the ends of the columns all reach 20MPa, indicating the concrete is already crushed, and the column ends have turned into plastic hinges.



(a) Loma_Prieta wave (at 11.2s)



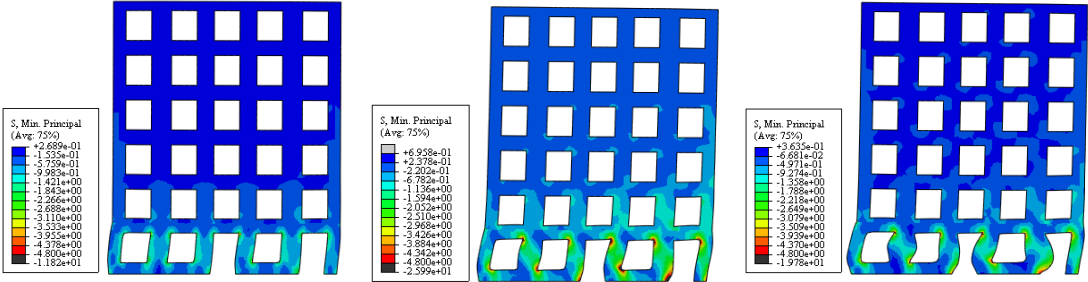
(b) El-centro_NS wave (at 10.47s)



(c) NorthRidge wave (at 8.0s)

Figure 5.5. Stress contours of the inner frame under three waves

Fig. 5.6 are the stress contours of the external walls under three earthquake waves at the onset of maximum stress in the wall. The figures show that the external walls of the first story and the walls between windows have all been damaged to some extent, where the maximum stress has reached the walls' compressive strength.



(a) Loma_Prieta wave (at 11.2s) (b) El-centro_NS wave (at 10.47s) (c) NorthRidge wave (at 8.0s)

Figure 5.6. Stress contours of the external walls under three waves

From the preliminary analyses, the maximum displacements of the structure, the order of plastic hinges, their location on the inner frame, and the distribution of the story drifts along the height are all similar under three waves. The maximum story drift is 0.002 at the first story as shown in Fig. 5.3. Through the paper we conclude that such type of structure's weak story is the first story, and its

seismic capability is insufficient to resist severe seismic loads.

6. CONCLUSION

In this paper, the dynamic characteristics under each damage state are obtained using free vibration method, and then used to update the finite element model, at last the seismic performance of the structure is analysed. From the preliminary work, such conclusion can be drawn:

- 1) A method to update the finite element model based on measured dynamic characteristics is developed, which is verified by frequency comparison between model and reality under various damage states.
- 2) The impact test shows that natural frequency of the structure decreases when damage increases, but the change is not too big. On the contrary, with the damage increases, the damping ratio increases as well.
- 3) Results from the dynamic nonlinear analyses show that, for most of such structures the first stories are the weak stories, and their seismic capabilities are not sufficient to resist severe seismic loads.

AKNOWLEDGEMENT

The authors gratefully acknowledge the financial support provided by the National Major Fundamental Research Program under grant Nos. 2007CB714202.

REFERENCES

- Zhou, X.Y. (2009). Research and practice of earthquake resistance of building structures for 60 years in China. *Journal of Building Structures* **39:9**, 1-14. (in Chinese)
- GB 50011-2010. (2010). Code for seismic design of buildings, China Architecture & Building Press, Beijing, China. (in Chinese)
- Hou, S., Zhang, H.B. and Yu S. (2011). Piezoceramic-based smart aggregates for seismic stress monitoring of RC building. *Proc. SPIE 7981*, 79812N.
- Clough, R.W., Penzien, J. (2010). Dynamics of Structures, Computers and Structures, USA.
- Mao, W.F. (2008). Seismic evaluation of single existing urban structures, Harbin Institute of Technology, Harbin, China. (in Chinese)
- GB 50010-2002. (2002). Code for Design of Concrete Structures, China Architecture & Building Press, Beijing, China. (in Chinese)
- Zheng, N.N. (2010). Research on Seismic Behavior of Masonry Structures with Fabricated Tie-columns, Chongqing Technology, Chongqing, China. (in Chinese)